Low Velocity Bird-Like Impact Behavior on Honeycomb Composite Structure

(Author(s)): Okan ÖZTÜRK[1], Faruk ELALDI[2]

ORCID[1]: 0009-0006-5678-730X

ORCID[2]: 0000-0003-0592-6868

Low Velocity Bird-Like Impact Behavior on Honeycomb Composite Structure

Highlights

- ❖ *Low-velocity impact*
- ❖ *Bird strike*
- ❖ *Rubber impactor*
- ❖ *Honeycomb structure*
- ❖ *Drop weight*

Graphical Abstract

In this study, the low-velocity impact response of a honeycomb sandwich composite which is produced for a typical unmanned air vehicle (UAV) was studied both experimentally and numerically.
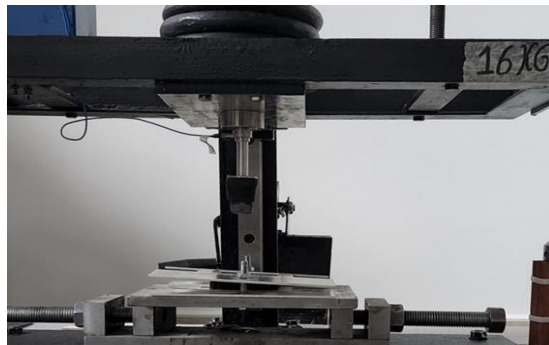

Figure. Drop weight test setup

Aim

This study aims to understand honeycomb structure behavior against to bird-like impact.

Design & Methodology

380 Joule, 276 Joule, and 224 Joule kinetic energies were applied to the honeycomb samples with rubber impactors of similar density, to simulate bird impact events. According to the laboratory boundary, an Ansys dynamic explicit model has been created and compared.

Originality

Investigation of the low-velocity impact of a bird-like impact behavior on composite structure.

Findings

In the experiments, it has been determined that the rubber-tipped impactors behave nonlinearly and become more rigid with increasing impact energy and, accordingly, the increase in displacement was not linear. Therefore, rubber-tipped impactors can be used for bird strike analyses.

Conclusion

This study proves that the composite sandwich panel that is used during the experimental test won't be heavily damaged by a rubber that has 165 grams of weight and 68 m/sn velocities.

Declaration of Ethical Standards

The author(s) of this article declare that the materials and methods used in this study do not require ethical committee permission and/or legal-special permission.

Low-Velocity Bird-Like Impact Behavior on Honeycomb Composite Structure

Araştırma Makalesi / Research Article

Okan ÖZTÜRK[1], Faruk ELALDI[1*]

[1]Mechanical Engineering Department, Baskent University, Türkiye

ABSTRACT

Composite materials are widely used in primary aerospace structures such as wing components and fuselage panels; however, their major disadvantage is their vulnerability to transverse impact loads that can lead to internal delamination and fiber/matrix separation. In this study, the effect of a low-velocity impact which simulates bird impact on a honeycomb sandwich composite plates produced by a co-curing technique for a typical unmanned air vehicle (UAV) was studied both experimentally and numerically. The surface plates of the composite samples were produced from carbon fiber/epoxy prepreg material. Nomex honeycomb core material was used to make the composite sandwich structure via an autoclave process. For the bird-like impact test, the tip of the impactor was coated with thick, tough rubber to simulate a bird strike; the diameter of the impactor was 25 mm to ensure similarity with a bird called Pica nuttalli (magpie), which has a mass of 155 g and is the closest bird body to the simulations. Three different predetermined impact scenarios with kinetic energy 380 Joule, 276 Joule, and 224 Joule were applied to the samples with rubber impactors of similar density, to simulate bird impact events with different impact directions. The impact behavior was characterized by velocity-time, force-time, and displacement-time graphs. Different levels of damage were observed in the composite samples, but none of the sandwich test samples were perforated, and it could therefore be concluded that the unmanned air vehicle could land without risk to flight safety. Ultrasound, digital microscope, and tap inspections have been applied for test samples to determine damage area size and types. This low-velocity bird-like impact was also modeled and analyzed using Ansys numerical program to verify the results, and it was concluded that the verified model could also be used for the preliminary design verification of dynamic bird-impact tests within the 10% sensitivity range.

Keywords: Low-velocity impact, sandwich panel, honeycomb.

Petek Yapılı Kompozit Malzemelerin Düşük Hızda Kuş Benzeri Darbelere Karşı Davranışı

ÖZ

Bu çalışmada, bir hava aracının kalkış ve inişlerinde meydana gelebilecek kuş çarpma olaylarında bal peteği (honeycomb) yapılı kompozit yapıların hasar davranışı hakkında deneysel ve sayısal çalışmayı öngören bir araştırma sunulmaktadır. Hava araçlarında sıklıkla kullanılan kompozit malzemelerin düşük hızlı çarpma sonucunda perfore olmaması yani hava aracı içine ulaşmaması beklenmektedir. Kompozit malzemede düşük hızlı çarpma davranışını ve meydana gelen hasar tiplerini incelemek amacıyla 75mm x 75 mm ölçülerindeki bal peteği yapılı kompozit numunelerin yüzey plakaları prepreg karbon fiber malzemeden üretilmiştir. Kompozit malzemenin alt ve üst yüzey plakaları eşit kalınlıktadır. Kuş çarpmasını kısmen simüle edecek impektör uç kısmı 25 mm çapında ve kuş çarpma deneylerinde kullanılan impektör geometrisine uygun şekilde küresel kauçuk malzemeden imal edilmiştir. Kauçuk impektör ile kompozit malzemeye 380 joule, 276 joule ve 224 joule' lük üç farklı düzeyde enerji seviyesi uygulanmıştır. Numune yüzeylerinde gözlemlenen hasarlar, hız-zaman, kuvvet-zaman, deplasman-zaman, enerji-zaman ve deplasman-enerji grafikleri ile karakterize edilmiştir. Ansys sayısal modelleme programı kullanarak yapılan sayısal analizlerle deneysel sonuçlar mukayese edilmiş ve hasar yüzeyleri incelenmiştir. Deneysel ve sayısal çalışmaların sonucunda birbirine yakın neticeler elde edilmiştir. Elde edilen model %10 maksimum sapma ile statik ve dinamik testlerin ön tasarım doğrulamasında kullanılabilecektir.

Anahtar Kelimeler: Sandviç yapı, kompozit, darbe, kuş çarpması, sayısal modelleme.

1. INTRODUCTION

The use of honeycomb composite materials in aircrafts becomes more common day by day. Accordingly, damage scenarios in honeycomb composite materials and their effects are investigated by researchers. Bird strike effects are considered to be one of the most important impact situations among these scenarios. According to the data of the Federal Aviation Administration (FAA), 276,846 accidents were reported in the United States alone due to the collision of birds and similar animals with aircrafts [1]. According to these numbers, 96% of the accidents occurred during take-off of the aircraft. The most important purpose of the EASA

---

and FAA bird impact test standards are to be strong enough to prevent bird particles from reaching the interior of the aircraft. Isabel et al., have conducted studies comparing the requirements of FAA and EASA bird strike certification [2]. Furthermore, they researched the serious risks of collisions between birds and aircraft in aviation. They mentioned airport and aircraft operations and how they affect the efficiency of the air traffic management system. Their research focuses on how to reduce risks and the potential of accidents with aircraft-mounted systems as well as regulations.

Aniello el at. researched a numerical investigation of the bird impact on a regional aircraft wing [3]. They evaluated the bird impact on real aeronautical structures. In their research, three different numerical approaches (Rigid Bird Model, Lagrangian Model, and SPH Model) were presented and compared. The results, as expected, showed a variable output in terms of wing indentation provided by the different approaches. The Lagrangian approach has been found to be the less computationally effective one. Hedayati and Ziaei-Rad studied in their analysis using the hemispherical cylinder bird model and different SEA methods, stated that Lagrange, Euler, and SPH methods gave approximate results and were compatible with the test results [4]. Saribas and Karadeniz, investigated the robustness of a wing leading edge against a possible bird strike [5]. Catia V5 program was used to create 3D modeling of wing and bird structures. SPH method was used to create the particle structure of the bird. Multiple simulation models have been developed for bird and wing structures, to compare the results from each simulation. According to the results, the strength of aluminum alloys is insufficient against high-speed bird impacts. Tatlier created a model to use the smooth particle hydrodynamics (SPH) model to conduct a bird strike effect on the leading edge of an aircraft wing [6]. Birds strike at the leading edge of the wings from different orientations, and bird strike simulations have been performed with various orientations. The bird approaching angles is illustrated for angles of 0°, 15°, 30°, 45°, 60° and 90° consecutively. No significant differences in the deformation of wing leading edge are returned by the simulations performed in Tatlier's study.

The bird-strike response of sandwich composites has been investigated by many researchers. James and John were some of the first researchers to conduct experimental studies analyzing different parameters [7-8]. Janusz et al. conducted research on efficient numerical tools for designing bird strike-resistant aircraft by revealing the impact behavior of the bird model with experiments in the laboratory environment [9]. They created a numerical model to reduce the cost and speed up the design process. The impactor was an elastic and the effects of the parameters on bird strike were found with the regression equations obtained from Minitab. Georgiadis et. al [16] used moveable trailing edge (MTE) and developed a methodology to support the bird-strike certification of the carbon fiber epoxy

(acrylic glass) material produced at 1.81 kg weight, 106 mm diameter, and 212 mm length per National Aeronautics and Space Administration (NASA) standards TN-2015-218340. It was determined that the bird models (gelatine) produced in the experiments were completely crushed like a liquid as a result of impacts and showed hydrodynamic behavior. Accordingly, it has been revealed in the impact tests that the amount of contact force applied to deformable (acrylic glass) targets under the same impact conditions is higher than the contact force applied to rigid materials. Liu et al. performed a crash test of a 1.8 kg dead chicken against the test sample at a speed of 150 m/s in order to examine the effects of bird strikes on the aircraft nose sidewall. As a result of the impact test, it was reported that perforation occurred in the material [10]. Michele et al. investigate experimental and numerical studies about bird impact strikes on airplane surfaces [11]. They created a bird finite model (FE) based on Lagrangian-Euler (ALE) principles. They prepared numerical models to compare against theoretical and experimental values. Liu et al. [12] conducted bird impact tests by throwing dead chickens weighing 1.8 kg onto a flat plate at speeds of 70, 120 and 170 m/s. They analyzed the 13.25 mm long hemispherical cylinder bird model using SPH and Murnaghan equation and showed that the analysis results were compatible with the test results. Sun et al. [13] have investigated the effects of structural parameters of honeycomb sandwich panels, namely face sheet thickness, core height, cell size, and cell wall thickness. A series of low-velocity impact tests with different initial energies were carried out by utilizing an instrumented falling-weight impact machine with a hemispherical impactor. Low-velocity impact tests on sandwich specimens were carried out using a drop-weight impact facility (INSTRON CEAST 9350). The impact tests were conducted at four impact velocities of 5.8 m/s, 8.3 m/s, 10.2 m/s, and 11.8 m/s, resulting in impact energies of 92.2 Joule, 188.8 Joule, 285.2 Joule, and 381.7 Joule, respectively. Two deformation and failure modes of sandwich panels are identified in response to low-velocity impact. The damage of both face sheets and core concentrated around the impact region, is dominated by localized indentation. The second type of damage occurred by the wrinkling of the front face sheet, bulging of the back face sheet, and overall crushing of the core, due to the global bending effect. Mahesh et al. [14]conducted research on the relative between absorbed energy, core density and applied energies. Hasilci and Bogoclu [15], used in their research the central composite design method one of the first applications in the bird strike problem. Bird strike simulations were performed in different analysis parameters based on the central composite design method composite, moveable trailing edge (MTE) of the Boeing 787 Dreamliner employing SPH model. SPH models are highly effective in modeling bird strike incidents because of its capability of modeling the high distortion and deformation with a smaller computation cost. Ergene

and Yalcın [17] investigated a research in their analysis by modeling composite materials through the Ansys program, they revealed which types of damage symbolize the shape changes in honeycombs as a result of the impact. Sen and Pakdil [18] have investigated the effect of stacking sequences on the failure behavior of pinned composite plates. To observe the influences of joint geometry and stacking sequence on the failure mechanism, failure analysis were carried out experimentally.

Beomkeun et al. research conducted on rubber-like materials shows hyperelastic characteristics representing elastic behavior in the range of large deformation, showing a nonlinear relationship between load and deformation [19]. Sebastian et al. modeled the rubber impactor according to the hyperelastic Mooney-Rivlin law. They revealed that 90% of the kinetic energy was stored in the elastic material after the impact [20]. Abrate studied about the impact of raindrops, hailstones, and birds on aerospace structures [21]. Dau et. al. investigated studies about the impact behavior of rubber. Low-velocity impact performed with 9.9 kg, 13.9 kg, and 17.9 kg mass velocity effect study are discussed. Force-time, displacement-time and force-displacement curves and damage mechanisms observed on micrographies were particularly commented [22]. Fard et. al. research about mechanical properties of rubber impactors with different materials under low-velocity impact [23].

Balaban et al. studied the impact behavior of sandwich composite beam structures manufactured by the vacuum-assisted resin infusion process. They observed that, according to the different energy levels, the impactor caused damage in the upper facesheets in the core materials, or stopped in the lower facesheets. It was seen that the impact damage area increased with the increase in impact energy level [24]. Ozsoy studied ply number and impactor geometry effects of carbon fiber reinforced epoxy composites were investigated by low velocity impact tests. Drop weight impact tests were carried out at 6 Joule, 12 Joule and 24 Joule energy levels by using hemispherical impactors with 10 mm and 20 mm diameters. Laminated composites were manufactured in 6, 10 and 14 plies with vacuum infusion method. The effects of laminate thickness, impactor diameter and impact energy on the contact force, velocity, absorbed energy and damaged surfaces were investigated and evaluated. It is observed that impactor geometries and velocities caused the different damage mechanisms [25]. Sahin et al. conducted research about effect of mass of the impactor upon the dynamic response of laminated composites. For this purpose, two different impactors with different masses were used. The impact velocities were selected so that impactors with different masses had the same kinetic energy. The experiments were performed on simply supported woven E-glass reinforced epoxy laminates which are made of 8 layers stacked symmetrically. The variation of impact force, impactor velocity, and laminate displacement versus interaction time were obtained. The impulse and energy absorption

characteristics and damage zones were also investigated [26]. Evran conducted studies about the effects of fiber orientation angles on the deflection analysis of the laminated composite plates were investigated using finite elements. Fiber orientation angles were modeled using the finite element software ANSYS [27].

Wojciech et al. studied the analysis of selected parameters in the numerical modeling of low-velocity impact damage in composite structures. According to the simulations carried out, it was concluded that the biggest cause of the results was the mesh density. Another highlighted point is von Misses stress; the biggest differences were obtained when comparing the different ways of modeling the composite plate. In the case where the plate was modeled as one layer, the maximal value of von Misses stress is more than two times higher than in the case of modeling the composite plate as 10 separate layers. Differences in the obtained results may be caused by not taking into account the delamination process occurring during impact [28].

In this study, the low-velocity bird-like impact effect on honeycomb sandwich composite plates, produced by a co-curing technique for a typical unmanned air vehicle (drone), was studied experimentally and numerically. The most common type of damage in landing and take-off of air vehicles is damage caused by bird strikes. Although there are too many experimental studies carried out on this subject in the literature, there are very few numerical model studies verified with experimental data in honeycomb composite materials. The aim of this study is to analyse the severity of bird strike for different scenerios and is to see how rubber-tipped impactor simulates the real bird impact. For this, three different energy levels of 380 J, 276 J, and 247 J based on three different impact angle were applied to the composite sandwich material test specimens. While those applied kinetic energies were selected, three different scenarios were taken into account. First, the impact occurred when the male magpie, weighing 165 grams [29], and the drone were flying toward each other, where the relative speed is 68 m/s (134 knots), and about 380 J of kinetic energy is applied to the drone structure. In the second scenario, when a female magpie, weighing 145 grams, impacted on drone from the side surface, the relative speed is 61 m/s (120 knots), and a kinetic energy of about 276 J is applied to the UAV structure. In the third scenario, when a 145-gram female magpie bird and the UAV were flying in the same direction with a relative speed of 54.5 m/s (106 knots), a kinetic energy of approximately 224 J was applied to the UAV structure.

2. MATERIAL AND METHOD

For the honeycomb composite samples used in this study, the vacuum bagging method was used by 13 layers of prepreg carbon fiber prepreg with orientation angles of [0°,-45°,+45°,0°,90°,0°,+45°,-45°,0°]. The composite material production process consists of two stages. The first stage is the preparation of the materials, and the

second stage is the autoclave process. While prepreg materials are bonded according to the given orientation, they are subjected to pre-vacuuming to prevent air gaps that may occur between the layers. For this purpose, the vacuum process was carried out from two points on the surface plates, while the applied pressure was controlled by connecting a manometer at one point. Thus, 760 mmHg of vacuum was applied to the upper and lower surface plates for 15 minutes before core placement to prevent the formation of pores in the plate. After this process, the honeycomb core was combined by applying an adhesive film to the bottom and top surface plates. After honeycomb placement, a 250 mmHg vacuum was applied to avoid problems such as gaps, pores, or non-adhesion. Vacuum leakage in the autoclave (no leakage greater than 9.75 mmHg within 10 minutes) and temperature control were carried out via manometer and thermocouple. Figure 1 shows the otoclave process of the sandwich composite.

Figure 1. Autoclave progress

The vacuum bagging method is based on the principle of placing the prepregs on a mould with a mould release agent in accordance with the determined layer sequence, isolating these prepregs from the external environment by means of putty tapes placed around the mould and vacuum bag, and preparing the structure for autoclave process by vacuuming. The autoclave process was carried out at 180 °C under a pressure of 0.3 MPa (using nitrogen gas) for 120 minutes. For the experiments, 50 mm x 50 mm samples were cut and prepared with the router bit. Physical and mechanical properties of the sandwich composite are shown in Table 1 and Table 2.

Table1. Physical and mechanical properties of the core honeycomb

Stabilized Compression (MPa)	L Shear Properties		W Shear Properties	
	Strength (MPa)	Modulus (MPa)	Strength (MPa)	Modulus (MPa)
1.72	1.06	35.85	0.57	19.3

Table2. Physical and mechanical properties of the faceplates

0° Tensile Strength (MPa)	0° Tensile Modulus (MPa)	90° Tensile Strength (MPa)	90° Tensile Modulus (MPa)
868.73	61	786	57.84

Ultrasound examination of the samples were performed prior to testing and no defects were found. The ultrasound results are shown in Figure 2. The darkening visible in the lower left corner of the material shows the ultrasound probe.

3. TESTING AND INSPECTION

Tests were carried out using a low-velocity impact device with the impactor covered with spherical rubber material. Bret et al. studied the flight kinematics of *Pica nuttalli*. Accordingly, they revealed that at flight speeds of 6 m/s and below, the bird's head position is ahead of its wings [30]. The bird shape is assumed to be a hemispherical-ended cylinder. Barber et. al. [31] investigated numerous bird species to come up with a bird density to be demonstrated density of 950 kg/m3. Therefore, the impactor diameter was taken at 25 mm in order to simulate bird-like impact. Depending on the three different impact scenarios determined, 380 J, 276 J, and 224 J of kinetic energy were applied to the samples with rubber impactors of similar density in terms of simulating the bird impact event. The same rubber impactor was used in all tests to ensure that the test results were not affected by the material structure of the rubber impactor.

The force applied to the surface during the impact process was measured by the load cell. The velocity of the impactor tip is measured by a linear variable differential transformer (LVDT) sensor connected to the system. LVDT is a magnetic position transducer for linear displacement measurement, and as it offers high resolution, accuracy, and good repeatability, is widely used in tests. For the measurement of the displacement with an LVDT, two secondary coils are connected differentially, and the voltages at the free ends of the two coils are measured. When the position of the core is shifted from the center, the output voltage appears proportional to the displacement of the core with 1% variation [32]. The variation of displacement force and velocity with time was recorded with computer data, and force-time, velocity-time, displacement-time, energy-displacement, and energy-time graphs were drawn in light of these data.

Fiber separation, matrix cracking, and delamination were observed on the top plate of the sample with an impact energy of 380 J, however, perforation did not occur, and the impactor rebounded. During visual inspection, damage was detected on a very large portion of the top plate with the honeycomb. The honeycomb was broken in most areas, and debonding was observed on the upper surface plate. This damage has been confirmed by

ultrasound tests. The ultrasonic scanning test results of the 1:1 scaled samples are shown in Figure 3a. The black areas show broken honeycomb areas. Damage occurred on the entire 56.25 cm² total area of the sample; however, perforation was not observed in the sample. The tapping test result of the sample is shown in Figure 3b.

For the 276 J impact energy, the ultrasound and tapping inspections, shown in Figure 4, have revealed that damage occurred on 42.0 cm² of the composite panel, accounting for approximately 75% of the specimen area. Ultrasound and tapping inspections for the impact energy of 224 J, shown in Figure 5, showed that approximately 60% of the honeycomb cell is deformed.
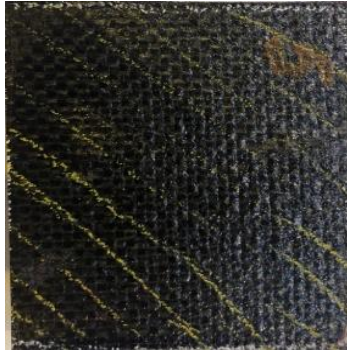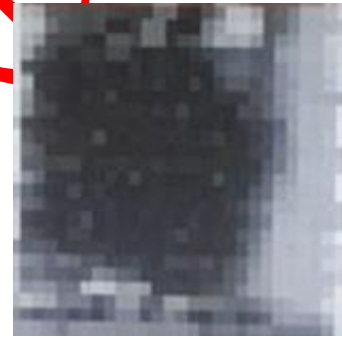

(a)   (b)

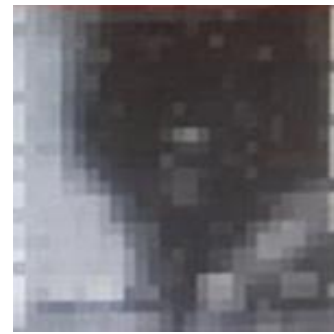**Figure 3.** Impact test with 380 J: a) tapping test result and b) ultrasound test result.

(a)   (b)

Figure 4. Impact test with 276 J: a) tapping test result and b) ultrasound test result.

(a)   (b)

Figure 5. Impact test with 224 J: a) tapping test result and b) ultrasound test result.

4. EXPERIMENTAL RESULTS

Based on the data obtained for 380 J, 276 J, and 224 J, impact characteristics such as contact force-time, velocity-time, and displacement-time graphics were plotted.

Force-time graph responses give qualitative indications on how the composites respond and whether any damage has taken place, and it is good predictor for evaluation.

Figure 6 shows the force-time history of a sample that has been tested at the energies of 380 J, 276 J, and 224 J.

The peak contact forces under 380 J impact energy were measured as 4.4 KN. The change in the slope of a load-time plot exhibits multiple occurrences of localized damage. Moreover, the smoothness and symmetry of a curve provide qualitative information about the damage. While the amount of force tends to increase, an increase in the slope of the graph is observed at 0.04 seconds after the impact. At this time, it is determined that damage has occurred on the upper surface plate. Then, the amount of force applied to the surface increased with an increasing slope, and a slope change occurred in the graph at 0.06 seconds after the moment of contact. At this moment, the honeycomb is considered to be damaged and broken. The contact force reached its peak point at 0.08 seconds after the first contact of the impactor. The force applied between 0.06 and 0.08 seconds from the moment of first contact was absorbed by the sub-surface plate. Perforation did not occur because the impact force could not overcome the fracture resistance, although the impactor penetrated the sub-surface plate. When the samples were checked as a result of the experiment, the upper surface plate and honeycomb damage were observed, and the lower surface plate had an impact pit.

In the graph of the impact test performed with 276 J of kinetic energy, the slope decreases at 0.04 seconds after the impact. At this time, it is determined that damage has occurred on the upper surface plate. A change in the slope of the graph is observed again at 0.06 seconds after the first contact. It is estimated that damage to the honeycomb occurs at this time. The contact force reached its peak point as 3.75 KN at 0.08 seconds after the first contact of the impactor. The force applied from the breaking of the honeycomb to the moment when the amount of force reaches its peak was covered by the lower surface plate; however, since no change was observed in the slope of the graph, penetration into the sub-surface plate did not occur. When the sample was checked, damage was detected on the upper surface plate and honeycomb, but no damage was observed on the lower surface plate.

According to the graph of the impact test performed with 224 J of kinetic energy, while the amount of force tends to increase, a change in the slope of the graph is observed at 0.04 seconds after the impact. At this time, it is determined that damage has occurred on the upper surface plate. Then, a slope change occurred in the graph at 0.06 seconds after the moment of contact. At this moment, it has reached a peak force point of 3.5 KN. This is the most important signal of honeycomb damage. After this moment, the slope of the graph showed a decreasing trend after going horizontal for a while. This indicates that the incoming force is countered by the sub-surface plate and rebounded.
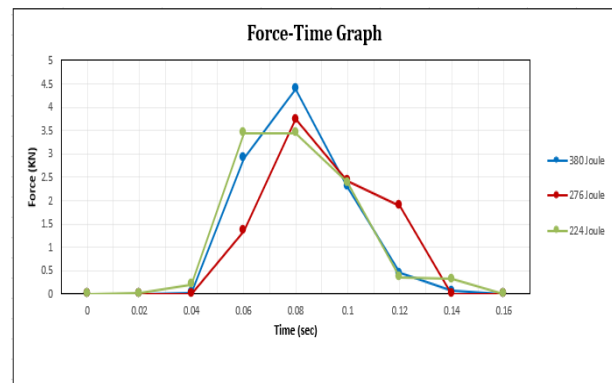

Figure 6. Force-time graph.

The velocities at the time of impact to the surface were measured as 4.36 m/sec, 4.04 m/sec, and 3.81 m/sec for 380 J, 276 J, and 224 J of kinetic energy, respectively (shown in Figure 7). The speed of the impactor reached its peak just before the impact, after which the velocity suddenly fell to zero.
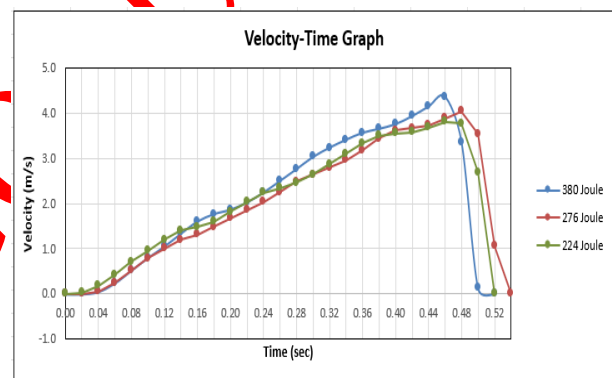

Figure 7. Velocity-time graph.

Comparing the force-time and velocity-time graphs, we can determine that the change in the slope of the graphs corresponds to the initial occurrence of matrix cracks. Before the first peak of impact velocity, there are no matrix cracks and no delamination extension, except for the presumed first minor delamination.

Figure 8 shows the displacement-time graph created with the data obtained in the experiment. According to the graph, as expected, the maximum displacement was recorded as a result of the impact of the impactor with 380 J of kinetic energy, which was measured as -30.28 mm. In the impact tests performed with 276 J and 224 J of kinetic energy, the displacement amounts of -28.18 mm and -25.10 mm, respectively, were measured. No other peak formation occurred in the graphs after the measured maximum values.
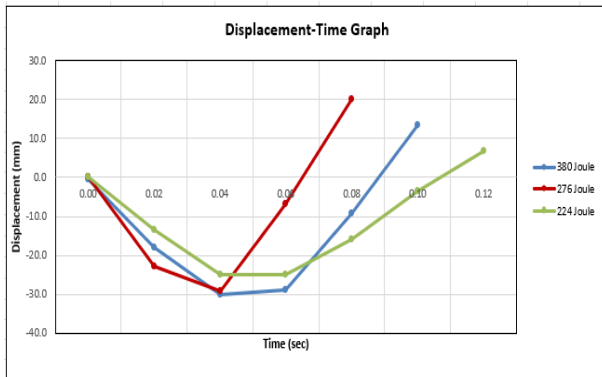
Figure 8. Displacement-time graph.

In order to calculate the amount of displacement occurring in the rubber impactor after the impact, 380 J, 276 J, and 224 J of kinetic energy were applied to the 40 mm thick steel plate through the rubber impactor in the laboratory environment. This thickness was chosen so that no displacement would occur on a steel plate. As a result of these experiments, the displacements on the rubber impactor were measured to be 26.47 mm, 25.6 mm, and 23 mm. The amount of displacement occurring in the rubber impactor increased depending on the amount of energy applied.

In order to measure the amount of bending deflection on the sandwich-structured composite materials, a flat ruler was placed on the surface hit by the impactor, a feeler gauge was placed to fill the gap between the composite material and the ruler, and the thickness of these felts was measured. These procedures were performed for all samples. In Figure 9 shown, the total amount of bending deflection of the sample was measured as 0.86 mm after the application of 380 J of kinetic energy. According to Figure 10, the total amount of bending deflection of the sample was measured as 0.76 mm after the application of 276 J of kinetic energy.
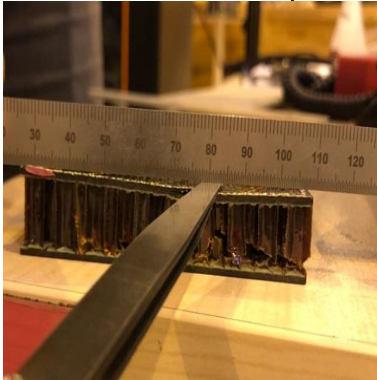

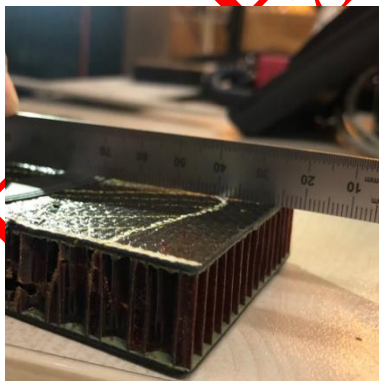**Figure 9.** Measurement of bending deflection after the application of 380 J of kinetic energy.

Figure 10. Measurement of bending deflection after the application of 276 J of kinetic energy.

Figure 11. Measurement of bending deflection after the application of 224 J of kinetic energy.

In Figure 11 shown, the total amount of bending deflection of the sample was measured as 0.26 mm after the application of 224 J of kinetic energy.

In Table 3, it is seen that most of the displacement is covered by the rubber impactor in the experiments where 380 J, 276 J, and 224 J of kinetic energy were applied. Therefore, the net penetration depth is calculated as 3.81 mm, 2.40 mm. and 2.10 mm respectively.

Table 3. Detailed displacement on the composite panels

	Total displacement (mm)	Penetration (mm)	Rubber impactor displacement (mm)
380 Joules	30.28	3.81	26.48
276 Joules	28.18	2.4	25.6
224 Joules	25.1	2.1	23

5. NUMERICAL ANALYSIS

In numerical solution, the model was completely simulated in ANSYS Dynamic Explicit. While determining the kinetic energy amounts to be applied to the sandwich composite samples, same scenarios studied in the experimental environment were taken into account in numerical modeling. According to this:

- The impact occurred when the male magpie, weighing 165 grams, and the drone were flying towards each other, where the relative speed is 68 m/s (134 knots), and about 380 J of kinetic energy is applied to the drone structure.

- When a female magpie, weighing 145 grams, impacted the drone from the side surface, the relative speed is 61 m/s (120 knots), and a kinetic energy of about 276 J was applied to the drone structure.

- When a 145-gram female magpie bird and the drone were flying in the same direction

with a relative speed of 54.5 m/s (106knots), a kinetic energy of approximately 224 J was applied to the drone structure.

In the numerical modeling calculations, the impact weight and velocity parameters were entered following those scenarios. The impact effects on the honeycomb composite structure by kinetic energies of 380 J, 276 J, and 224 J were analyzed by means of a rubber impactor with a diameter of 25 mm. In the initial state, the most defining feature is the impact velocity and weight of the impactor to be applied.
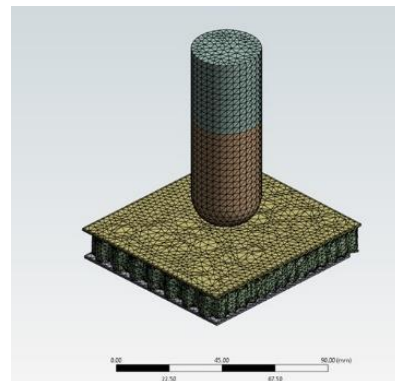

Figure 12. Numerical model mesh structure.

Figure 12 shows the numerical model mesh structure. The total number of elements in the composite material mesh structure with the impactor and honeycomb structure is 116438, and the number of nodes is 37223. Element type Tet4 was used in the masses simulating bird weight, the Hex8 element type was used in the lower and upper surface plates, and the Wed6 element type was used in the honeycomb. The boundary conditions of the modeling are as follows:

- The bottom surface of the honeycomb composite material was taken as fixed support since it was fixed to the ground in the experimental environment.

- By using the drop height application of the numerical program, it aimed to reach the impact speed of 68 m/sec by dropping the

rubber impactor, weighing 165 grams, from a height of approximately 240 meters. In Ansys dynamic explicit drop weight used during this analysis, velocity was given 0 m/sn. and 68 m/s measured on impact moment from impactor to sample.

- Utilizing a numerical model, the impactor of 145 grams is dropped from approximately 195 meters and 150 meters, and it aimed to reach impact speeds of 61 m/s and 54.5 m/s, respectively.

- Velocity is defined only in the y-axis direction of the impactor.

- Impactor targetted to the center of test samples.

- Sample fixed on edge to not slide during energy transfer. The numerical model also selected fixed support on edge points.

- Iteration has been applied for mesh density to get an optimized result on displacements. 4 mm, 4.1 mm, 4.2 mm, 4.3 mm, 4.4 mm, and 4,5 mm mesh have been applied to obtain the average displacement. iteration results are shown in Table 4.

Table 4. Mesh -Displacement iteration for 380 applied energy

380 Joule Iteration				
	Mesh Size (mm)	Displacement (mm)	Nodes	Element
	4	29.66	38534	119415
	4.1	31.38	37512	118146
	4.2	29.68	37362	116911
	4.3	33.80	37120	115820
	4.4	28.72	36679	114718
	4.5	27.95	36330	113616
Avarage	**4.25**	**30.20**	**37223**	**116438**

6. RESULTS AND DISCUSSION

The impact test and numerical model analysis results with 380 J, 276 J, and 224 J kinetic energy levels were compared in terms of contact force and total displacement amount. When the experimental results and numerical modeling results are compared, it is seen that the biggest deviation is the 1% in displacement obtained in the impact tests performed with 380 J of kinetic energy.
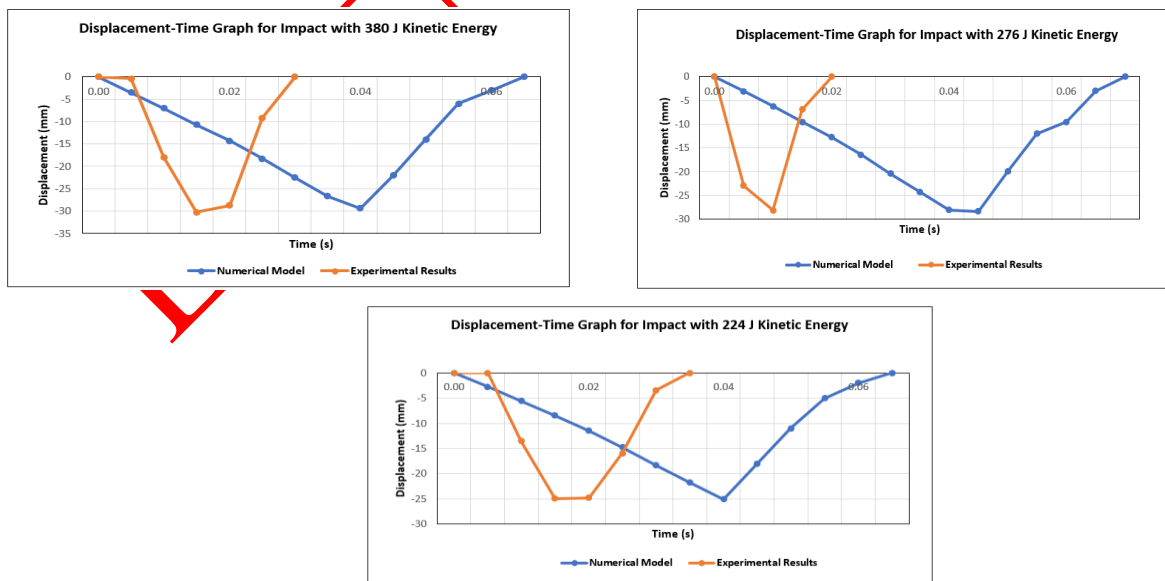

Figure 13. Displacement-time graph comparison of experimental results and numerical modeling results.

Figure 13 shows the comparison of displacement-time graphs drawn using data obtained from experimental tests and numerical modeling analysis for three different kinetic energy levels. The slope

of the displacement-time graph drawn with the data obtained from the test results and the slopes of the graph obtained through the numerical analysis method are consistent. The curves of the numerical solution are smoother and sharper than the experimental data curves. Since the amount of data received from numerical modeling per unit time is greater than the amount of data received through the LVDT sensor in the experiments, the numerical modeling graphics appear smoother. Depending on the determined scenarios, the amount of kinetic energy required in the study was calculated, and the value obtained was applied to the samples by changing the weight due to the limitations in the laboratory environment. Table 5 shows the comparison of numerical modeling and test results in terms of displacement amounts.

Table 5. Displacement comparison between experimental and numerical analyses

	Total displacement (mm)			Penetration (mm)			Rubber impactor displacement (mm)		
	Experimental	Numerical model	Deviation	Experimental	Numerical model	Deviation	Experimental	Numerical model	Deviation
380 Joules	30	30.20	0.01	3.7	3.5	-0.01	26.3	26.3	0.00
276 Joules	29.12	28.52	0.03	3.18	2.97	-0.07	25.73	25.55	0.00
224 Joules	26.44	26.83	0.01	2.13	2.15	0.01	24.31	24.68	0.01

In order to compare the types of damage as a result of the experiments, the damaged samples in laboratory tests were cut from the middle axis of the composite material, with the help of a computer numerical control (CNC) composite cutting machine, and the damages on the samples were examined. The damage caused by the impacts of the impactor with 380 J, 276 J, and 224 J of kinetic energy are shown in Figures 14a, 14b, and 14c, respectively. Accordingly, crushing and breaking were observed in the cells. There is a separation between the layers. When looking at the impact from 224 J of kinetic energy, it was determined that the amount of damage remained in a more limited region compared to other weight levels, but the same types of damage (cell crushing, cell and top plate separation, delamination) occurred.
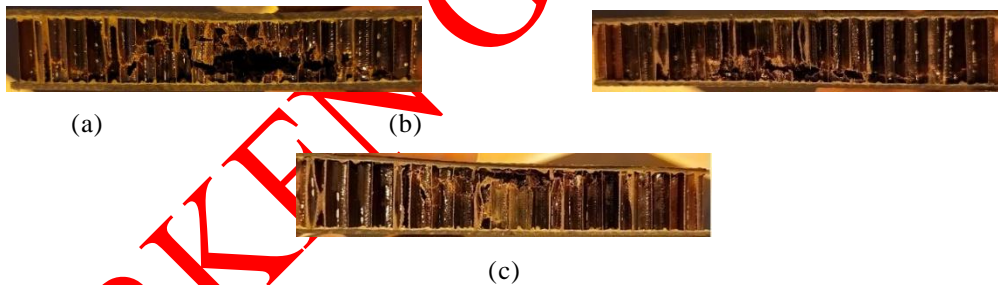

(a)   (b)

(c)

Figure 14. Damage caused by (a) 380 J, (b) 276 J, and (c) 224 J of kinetic energy

In Figures 15a, 15b, and 15c, the damage types revealed as a result of the numerical modeling analysis of the samples with 380 J, 276 J, and 224 J of kinetic energy applied, respectively, are shown. The experimental results and numerical modeling analyses show similarities in terms of the damaged areas. According to the numerical analysis, after applying 380 J, 276 J, and 224 J kinetic energies to composite materials, 0.92 mm, 0.79 mm, and 0.29 mm deflection bending occurred on composite part surfaces. In the experimental environment, 0.86 mm, 0.76 mm, and 0.26 mm bending deflection was measured as a result of applying 380 J, 276 J, and 224 J kinetic energy. Debonding has been observed between the upper surface and cell for each impact energy level. In the analysis results obtained as a result of applying 224 J of kinetic energy to the composite material surface in numerical modeling, less damage was observed compared to the 380 J and 276 J energy applications. As a result of the impact tests carried out in the experimental environment, it was determined that the bending displacement amounts measured on the composite material surface and shown in Figure 9, Figure 10, and Figure 11 were similar to the numerical analysis results shown in Figure 15.
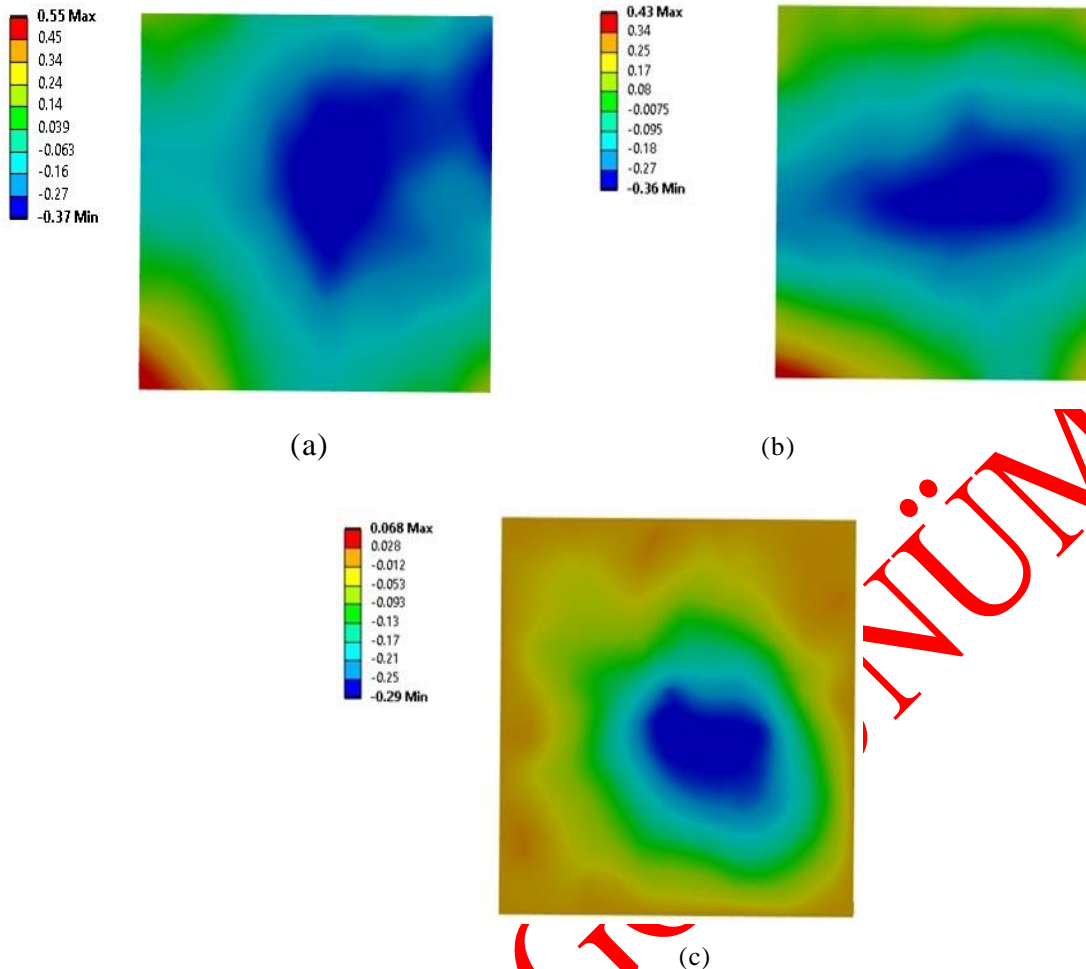
Figure 15. Numerical analysis of bending deflection on composite caused by (a) 380 J, (b) 276 J, and (c) 224 J of kinetic energy.

For the analysis of the low-velocity bird strike effect on the honeycomb composite material, a numerical bird-composite plate strike model was prepared by verifying with the experimental data. This model can be used with 10% accuracy to perform damage analysis in bird strikes of different speeds and masses. Since the numerical model was verified with experimental data, it was possible to run crash tests in different scenarios without using time and cost. Accordingly, in accordance with the EASA CS-25 bird impact test standard, the impact test of a bird weighing 1.8 kg to a typical unmanned aerial vehicle with a speed of 68 m/s was simulated by numerical model without changing the parameters of the prepared model. For example, the result of this analysis showed a total displacement of 52 mm, and although the top surface plate and honeycomb were completely damaged, no perforation occurred). The net displacement in the sandwich composite sample is approximately 8 mm, while the amount of displacement in the rubber impactor was measured as 44 mm. As a result of the numerical modeling analysis simulating the impact of a 1.8 kg bird with a composite material at a speed of 68 m/s, it was determined that the composite material behaved in accordance with EASA CS-25 standards and was not perforated.

7. CONCLUSION

In this study, the behaviour of honeycomb composite material against low-velocity impacts, such as bird strikes, was investigated. For this purpose, force-time, velocity-time, and displacement-time curves representing the characteristics of the composite material's response to low-speed impacts were drawn in light of experimental data. A rubber impactor was used to simulate bird strikes in a laboratory setting. The amount of displacement caused by the low-velocity impact, the amount of penetration, the impact velocity, and the amount of energy absorbed by the rubber impactor and sandwich composite material were found and shown with the help of graphics. The data obtained in the analyses made by creating a numerical model through the numerical program were compared with the experimental data, and results equivalent to the laboratory environment were found. The numerical model was validated with experimental data. Thanks to

the created model, the behavior of the honeycomb composite material against low-speed impacts can be used to analyze bird strikes of different sizes without further experimentation and cost and time losses.

As a result of the low-velocity impact, damages such as matrix cracks, fiber breaks in the upper surface plates, delamination, and cell crushing in the core have occurred in the samples. Types of damage were revealed by ultrasound, tap examination, and digital microscopes.

The outcomes of the experimental studies and numerical modeling were summarized as follows:

- As a result of the impact of the female magpie bird, weighing 145 grams and having speeds of 61 m/s and 54.5 m/s, to a typical unmanned aerial vehicle, perforation did not occur, and it was revealed that the drone could land without risking flight safety.

- Since the male magpie bird, weighing 165 grams and having a speed of 68 m/s, crashed into a typical unmanned aerial vehicle, it was determined that the drone could land safely without risking flight safety since perforation did not occur.

- It could be said that dent occurrences due to magpie-type bird strikes will not cause bird particles to reach the interior of the drone.

- In the experiments, it has been determined that the rubber-tipped impactors behave nonlinearly and become more rigid with increasing impact energy and, accordingly, the increase in displacement was not linear. Therefore, rubber-tipped impactors can be used for bird strike analyses.

- This study preliminary works of foreign object damage (FOD) which is a highist level risk for aviation. The Concorde plane accident (July 2000) occurred because of the impact of a rubber (FOD) which has been removed from the landing tire and posed a life-threatening risk. This study proves that the composite sandwich panel that is used during the experimental test won't be heavily damaged by a rubber impactor that has 165 grams of weight and 68 m/sn velocities.

- It was concluded that the resulting verified model can be used for preliminary design verification of dynamic bird-impact tests within the 3% sensitivity range.

- The created Ansys model allows for saving time, reduces cost, and also gives a chance to make studies with different scenarios like colder weather, pre-tensioned sample

behavior, and tests with different impactor materials.

DECLARATION OF ETHICAL STANDARDS

The authors of this article declare that the materials and methods used in this study do not require ethical committee permission and/or legal-special permission.

AUTHORS' CONTRIBUTIONS

Okan Öztürk: Performed the experiments, created to numerical model, and analyzed the results.

Faruk Elaldı: Performed the experiments, created to numerical model, and analyzed the results.

CONFLICT OF INTEREST

There is no conflict of interest in this study.

REFERENCES

[1] *www.faa.gov*, ''Wildlife-Strike-Report-1990-2022'' (2022).

[2] Isabel M, Joost E, Thorsten M, et al. ''The bird strike challenge'' *J. Aerosp.* MDPI, 7(3), 7–26, (2020).

[3] Aniello R, Roberta C, and Salvatore S. ''A brief introduction to the bird strike numerical simulation'' *Am. J. Eng. Appl. Sci.*, 9(4), 946–950, (2016).

[3] Hedayati, R., Ziaei-Rad, S. "A New Bird Model and the Effect of Bird Geometry in Impacts From Various Orientations", *Aerospace Science and Technology*, vol. 28, p. 9–20, (2013).

[5] Saribas M. F. ,and Karadeniz S., "Numerical Investigation of Bird Strike on an Aircraft Wing Leading Edge by Smooth Particle Hydrodynamics Method," *Gazi Journal of Engineering Sciences*, 8, (3): 547-566, (2022).

[6] Tatlier, M. S., ''A Numerical Investigation of a Bird Strike on the Structure of an Aircraft Wing Leading Edge'', *European Mechanical Science*, 4(1): 37-40, (2020).

[7] James W. ''Impact Behavior of Low Strength Projectiles; Technical Report AFML-TR-77-134'', *Air Force Materials Laboratory: Dayton,* OH, USA, (1977).

[8] John B, Henry T and James W. ''Bird Impact Forces and Pressures on Rigid and Compliant Targets; Technical Report AFFDL-TR-77-*60*'' *Air Force Flight NTIS.* OHIO, (1976).

[9] Janusz C, Ewelina K and Artur G. ''Experimental and Numerical Investigations of Bird Models for Bird Strike Analysis'' *Energies.* 15: 3699–3725, (2022).

[10] Liu J, Yulong L, Xiaosheng G, et al. ''Numerical model for bird strike on sidewall structure of an aircraft nose'' *Chinese J. Aeronaut.*, 27(3): 542–549, (2014).

[11] Michele G, Francesco M, Michele M, et al. ''Analysis of bird impact on a composite tailplane leading edge'' *Appl. Compos. Mater.*, 15: 241–257, (2008).

[12] Liu, J., Li, Y., Gao, X. "Bird Strike on a Flat Plate: Experiments and Numerical Simulations", *International*

Journal of Impact Engineering, 70: 21-37, (2014).

[13] Sun G, Huo X. , Wang H.,Hazel P. J.l, Li Q. ''On the structural parameters of honeycomb-core sandwich panels against low-velocity impact'' *Composites Part B* 216: 108881, (2021).

[14] Mahesh V., Mahesh V., Harursampath D., ''Low-Velocity Impact Response of the Composite Sandwich Panels'' *Sandwich Composites,* Edition1st Edition, CRC Press, 16, (2022).

[15] Hasilci Z., Bogoçlu M. E., ''Determining the effect of bird parameters on bird strikes to commercial passenger aircraft using the central composite design method'', *IJAA*, 2(1): 1-8, (2021).

[16] Georgiadis, S., Gunnion, A.J., Thomson, R.S., Cartwright, B.K.,'' Bird-strike simulation for certification of the Boeing 787 composite moveable trailing edge'' *Composite Structures* 86(1–3): 258–68.

[17] Ergene B. And Yalcin B., "Finite element analyzing of the effect of crack on mechanical behavior of honeycomb and re-entrant structures", *Politeknik Dergisi*, 23(4): 1015-1025, (2020).

[18] Sen F. and Pakdil M., ''Effect of Stacking Sequences on Failure Behavior of Pinned E-Glass/Epoxy Composite Plates'', *Journal of Polytechnic*, 11(2): 147-151, (2008).

[19] Beomkeun K, Seong L, Jayone L, et al. ''Comparison among neo-hookean model, moone, rivlin-model, and ogden model for chloroprene rubber'' *Int. J. Precis. Eng. Manuf.*, 13(5): 759–764,(2012).

[20] Sebastian H, Björn VDB, Yann K, et al. ''Rubber impact on 3D textile composites'' *Appl. Compos. Mater.*, 19: 275–295, (2012).

[21] Abrate, S., "Soft Impacts on Aerospace Structures", *Progress in Aerospace Sciences*, 81: p. 1–17,(2016).

[22] Dau F., Dano M.L., Kergomard Y. D., ''Experimental investigations and variability considerations on 3D interlock textile composites used in low velocity soft impact loading,'' *Composite Structures*, 153: Pages 369-379, (2016).

[23] Fard A. T., Khodadadi A., Liaghat G., Yao X.F., Mehrizi M.A.Z,'' Mechanical properties and energy absorption capacity of chopped fiber reinforced natural rubber.'' *Composites Part C*, 7: 100237, (2022).

[24] Balaban A., Kong T and Meltem T. ''Low Velocity Impact Behaviour of Sandwich Composite Structures with E-Glass/Epoxy Facesheets and PVC Foam'' *Procedia Struct.*, 18: 577–585, (2019).

[25] Ozsoy M. İ., ''Impactor Diameter and Ply Number Effects on the Impact Behavior of Carbon Fiber Composite Laminates'', *GU J Sci, Part C*, 10(3): 439-454, (2022).

[26] Sahin Omer S., Gunes A., Karadag H. B., ''Effect of Impactor Mass on Dynamic Response and Retention Properties of Composite Plates under Successive Impacts'', *CBU J. of Sci*., 12(1): p 27-37.

[27] Evran S., "Investigation of effects of fiber orientation angles on deflection behavior of cantilever laminated composite square plates", *Politeknik Dergisi*, 23(3): 633-639, (2020).

[28] Wojciech D, Andrzej K and Angelika K. ''Analysis of selected parameters in numerical modeling of low-velocity impact damage in composite structures'' *Procedia Struct*. 25: 19–26, (2020).

[29] Tim B. ''The Magpies: The Ecology and Behaviour of Black-Billed and Yellow-Billed Magpies'' *T & AD Poyser*, London, (1991).

[30] Bret T and Kenneth D. ''Flight kinematics of black-billed magpies and pigeons over a wide range of speeds'' *J. Exp. Biol.*, 199: 263–280, (1996).

[31] Barber, John P. ; Taylor, Henry R. ; Wilbeck, J.S., ''Bird impact forces and pressures on rigid and compliant targets'' *University of Dayton Ohio Research Institute*, (1978).

[32] Young-Soo Yang, Kang-Yul Bae, "The Modeling and Design of a Linear Variable Differential Transformer", *IJPEM,* 23: 153–162, (2022).